IL NUOVO CIMENTO Vol. 37 C, N. 2 Marzo-Aprile 2014
DOI 10.1393/ncc/i2014-11749-7

Colloquia: LC13

Beyond the SM with nonlinearly realized gauge theories

R. Ferrari
INFN, Sezione di Milano - Milano, Italy

ricevuto il 17 Febbraio 2014

Summary. — A Stückelberg Mass Term (SMT) is introduced in a $SU(2)$ non-abelian gauge theory as an alternative to the Higgs mechanism. A lattice model is used in order to investigate the mass spectrum of the theory, in particular the presence of Higgs-like bound states. Simulations indicate the presence of neutral bound states. Further investigations are needed in order to compare the model with experiments.

PACS 11.15.Ha – Lattice gauge theory.
PACS 12.60.-i – Models beyond the standard model.
PACS 13.85.-t – Hadron-induced high- and super-high-energy interactions.
PACS 14.80.Ec – Other neutral Higgs bosons.

1. – Introduction

The mass m is introduced in the action on the cubic lattice of size $N \equiv L^4$ with sites x and links μ

$$S_L = \frac{\beta}{2}\,\mathfrak{Re}\sum_{\square}\mathrm{Tr}\{1-U_{\square}\} + \frac{\beta}{2}m^2\mathfrak{Re}\sum_{x\mu}\mathrm{Tr}\Big\{1-\Omega(x)^{\dagger}U(x,\mu)\Omega(x+\mu)\Big\}, \tag{1}$$

where the sum over the plaquette is the Wilson action. $U(x,\mu), \Omega(x) \in SU(2)$ and in the naive limit of zero lattice spacing a one gets a mass term *à la* Stückelberg ($M^2 = a^{-2}m^2$)

$$S_{YM} + M^2\int \mathrm{d}^4x\ \mathrm{Tr}\left\{\Big[gA_\mu - i\Omega\partial_\mu\Omega^{\dagger}\Big]^2\right\}. \tag{2}$$

The Stückelberg term provides a mass for the vector mesons but renders the theory nonrenormalizable. Lattice simulation overlooks this problem, which is crucial in perturbation theory.

The lattice formulation allows the exploration of the nonpertubative regime (as large energy phenomena, bound states). The present work is devoted to this exploration. The missing link to phenomenology is the identification of the line in the parameter space $(m^2(a), \beta(a))$ which allows the evaluation of the physical amplitudes. This can be achieved either by: i) evaluate relation among physical amplitudes where the dependence from $m^2(a)$ and $\beta(a)$ has been removed; ii) go in the perturbative regime and compare the amplitudes evaluated in the lattice and in the continuum.

2. – Local and global gauge invariance

The action is invariant under the *local-left* transformations $g_L(x) \in SU(2)_L$ and the *global-right* transformations $g_R \in SU(2)_R$

$$SU(2)_L \begin{cases} \Omega'(x) = g_L(x)\Omega(x), \\ U'(x,\mu) = g_L(x)U(x,\mu)g_L^\dagger(x+\mu), \end{cases} \qquad SU(2)_R \begin{cases} \Omega'(x) = \Omega(x)g_R^\dagger, \\ U'(x,\mu) = U(x,\mu). \end{cases} \tag{3}$$

We would like to stress the importance of this invariance property, in particular because in the nonrenormalizable continuum Minkowskean theory it is the starting point for the removal of the ultraviolet divergences of the loop expansion [1, 2]. In fact the invariance of the path integral measure ensures the validity of the LFE for the generating functionals [3].

3. – Features of the lattice model

The statistics is performed by using the partition function

$$Z[\beta, m^2, N] = \sum_{\{U,\Omega\}} e^{-S_L} \tag{4}$$

It is well established that a Transition Line (TL) exists with end point at $\beta \simeq 2.2$ where energy and order parameter ($D = 4$) (see ref. [4] and references therein),

$$\mathfrak{C} = \frac{1}{DN\beta}\frac{\partial}{\partial m^2}\ln Z = \frac{1}{2ND}\left\langle \mathfrak{Re}\sum_{x\mu}\mathrm{Tr}\{\Omega^\dagger(x)U(x,\mu)\Omega(x+\mu)\}\right\rangle, \tag{5}$$

have an inflection point becoming steeper by increasing β. See fig. 1 The presence of a TL could be of paramount importance for high energy processes at LHC. One could compare Higgs mechanism models with Sückelberg mass term theories.

4. – Gauge invariant fields

We study the two-point functions which can provide some information on the spectrum. The gauge invariant fields are very useful (τ_a are the Pauli matrices).

$$C(x,\mu) := \Omega^\dagger(x)U(x,\mu)\Omega(x+\mu) = C_0(x,\mu) + i\tau_a C_a(x,\mu). \tag{6}$$

By construction

$$C(x,\mu) \in SU(2). \tag{7}$$

$C(x,\mu)$ is invariant under local-left transformations (3), while under the global-right transformations it has $I = 0$ (C_0) and $I = 1$ (C_a) components (I is the isospin). One has

$$C_0(x,\mu)^2 + \sum_{a=1,3} C_a(x,\mu)^2 = 1. \tag{8}$$

5. – Correlators: general properties

In the deconfined region we expect the global-right symmetry to be implemented and therefore

$$\begin{aligned} &\langle C_a(x,\mu)\rangle = 0, \\ &\langle C_a(x,\mu) C_b(y,\nu)\rangle = 0, \qquad if\ a \neq b. \end{aligned} \tag{9}$$

The equations in (9) are satisfied by the numerical simulations to a reasonable level of accuracy.

6. – Correlators: energy gaps

Consider the two-point function of the zero-three-momentum operator

$$C_j(t,\mu) = \frac{1}{L^{\frac{3}{2}}} \sum_{x_1,x_2,x_3} C_j(x_1,x_2,x_3,x_4,\mu)|_{x_4=t}, \quad j = 0,1,2,3. \tag{10}$$

Then we evaluate the connected correlator

$$C_{jj',\mu\nu}(t) = \frac{1}{L} \sum_{t_0=1,L} \Big\langle C_j(t+t_0,\mu) C_{j'}(t_0,\nu) \Big\rangle_C. \tag{11}$$

The correlator is zero unless $j = j'$ and $\mu = \nu$. The spin one- and zero- amplitudes V and S are extracted by using the relation

$$C_{jj,\mu\nu}(t) = V_{jj}(\delta_{\mu\nu} - \delta_{\mu 4}\delta_{\nu 4}) + S_{jj}\delta_{\mu 4}\delta_{\nu 4}. \tag{12}$$

Very good fit of the data is obtained by using the function

$$g(t) = \frac{1}{2}(f(t) + f(L-t)), \tag{13}$$
$$f(t) = b_1 e^{-m_1 t} + b_2 e^{-m_2 t}.$$

Two exponentials are needed only for $m \simeq m_c$, as we will illustrate shortly. Otherwise one single exponential is enough for the fit. For comparison the $\beta = 1.5$ single exponential is shown with the $\beta = 3$ two exponentials in fig. 2 and 3. For $\beta = 1.5$ fig. 4 shows the spectrum of the $I = 1$,$J = 1$ states (isovector spin 1 states), while fig. 5 represents the $I = 0$,$J = 0, 1$ states (isoscalar spin 0,1 states).

7. – The spectrum for $\beta = 10$

For β above the end point the fit with two exponentials becomes necessary as m^2 approaches m_c^2. Typically (clearer in the isovector channel) there is a bifurcation point where one gap follows the bare value m and the other is very large. A series of Figures illustrates the phenomenon: fig. 6 for $I = 1, J = 1$, fig. 7 for $I = 0, J = 0$, fig. 8 for $I = 0, J = 1$. The onset of bifurcation is a rather noisy spot, as the statistical errors show.

By m^2 approaching m_c^2 the weight of the large gap becomes dominant. These features are once more a distinct sign of the transition from the unconfined to the confined phase. It is particularly clear in the isovector-vector channel (gauge bosons). By approaching the TL the weight of the lower gap vanishes while the large gap become dominant. By crossing the TL the lower gap disappears and the correlation vanishes. This process occurs at the TL, that tends asymptotically to zero for $\beta \to \infty$. Thus in the limit the mass of the gauge bosons acquires more and more lower values before disappearance.

8. – Conclusions

Let us summarize the results of the lattice simulation of the lattice massive Yang-Mills regarding the spectrum.

i) No correlation in the $I = 1, J = 0$ channel

ii) Single exponential fit of correlators for $\beta < 2.2$ and for $m^2 >> m_c^2$. Bifurcation to two exponential fit for $m^2 \simeq m_c^2$.

iii) The $I = 1, J = 1$ gap follows close the bare value m.

iv) In the Källén-Lehmann representation the weight of the lower gap vanishes for $m \to m_c$

v) while in the same limit the higher gap dominates.

Further results on the spectrum has appeared in [5].

Outlook:further research will be focused on many interesting features of the model

1. Study the properties of the TL,
2. Understand the deviation of the vector meson mass from the bare value,
3. Examine the origin of the larger gap present after the bifurcation.

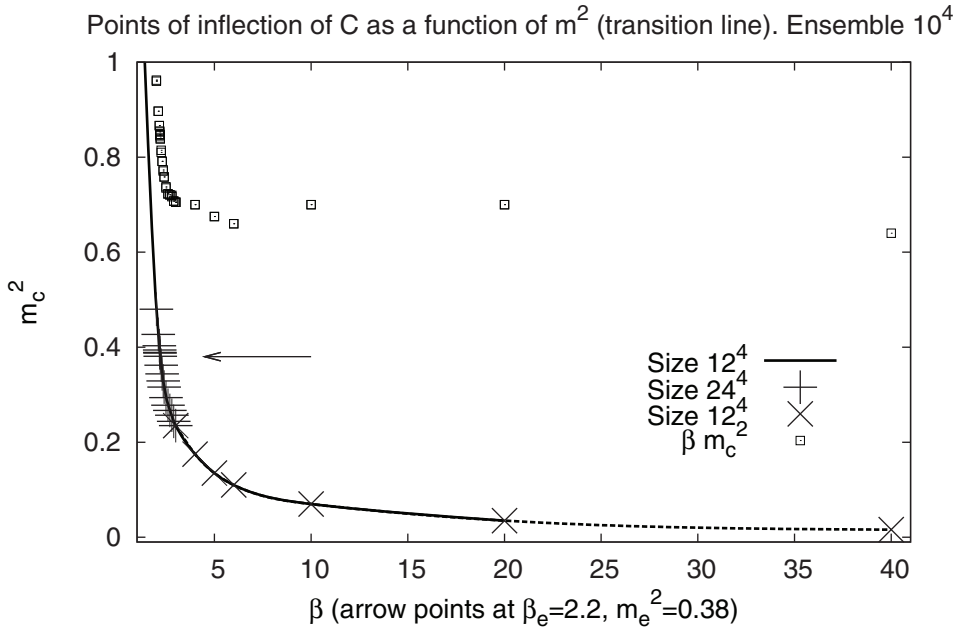

Fig. 1. – The transition line. The arrow marks the position of the end point.

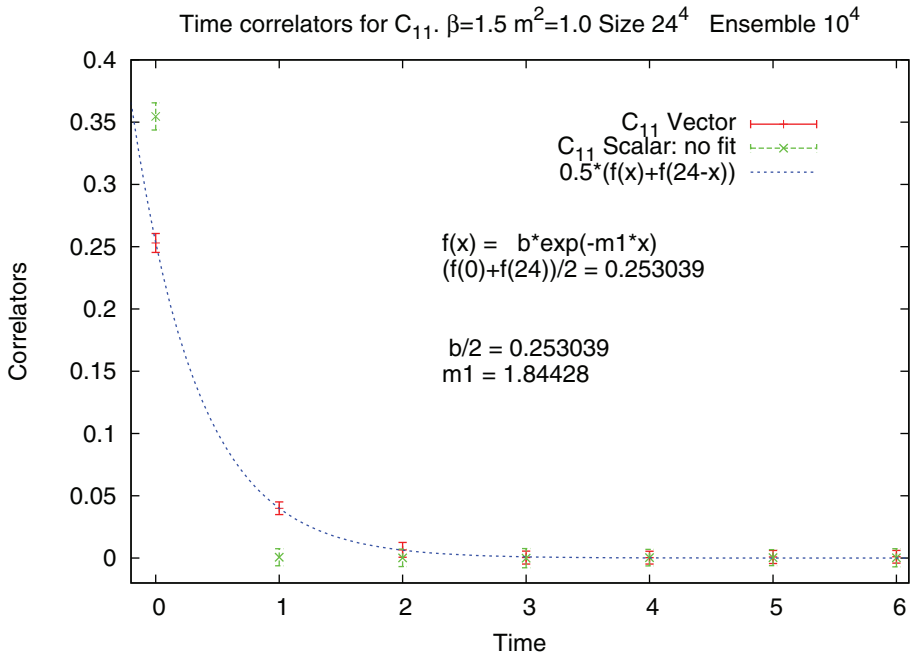

Fig. 2. – A time correlator in the isovector channel where a single exponential is used. The mass m^2 is close to the TL at $m^2_{\rm TL} \sim 0.9$.

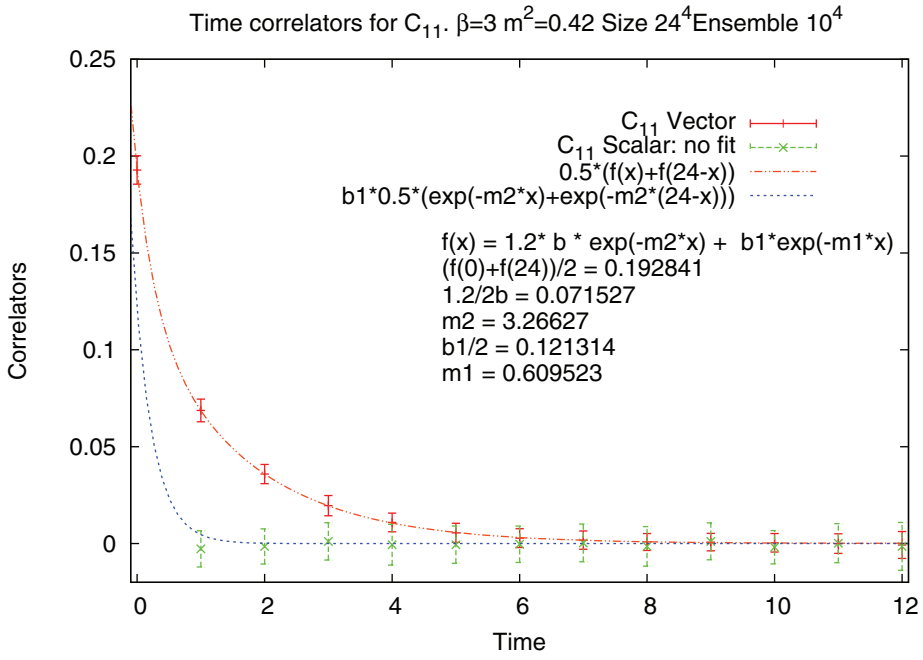

Fig. 3. – A time correlator in the isovector channel where two exponentials are used. The mass m^2 is close to the TL at $m_c^2 \sim 0.231$. The figure shows the contribution of the large energy gap.

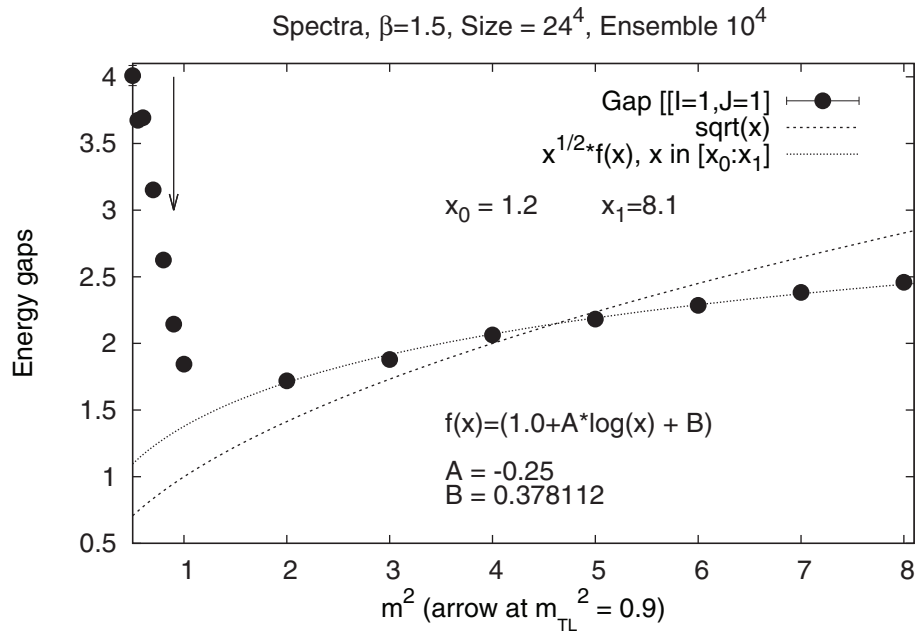

Fig. 4. – Mass spectrum of the gauge vector meson for $\beta = 1.5$.

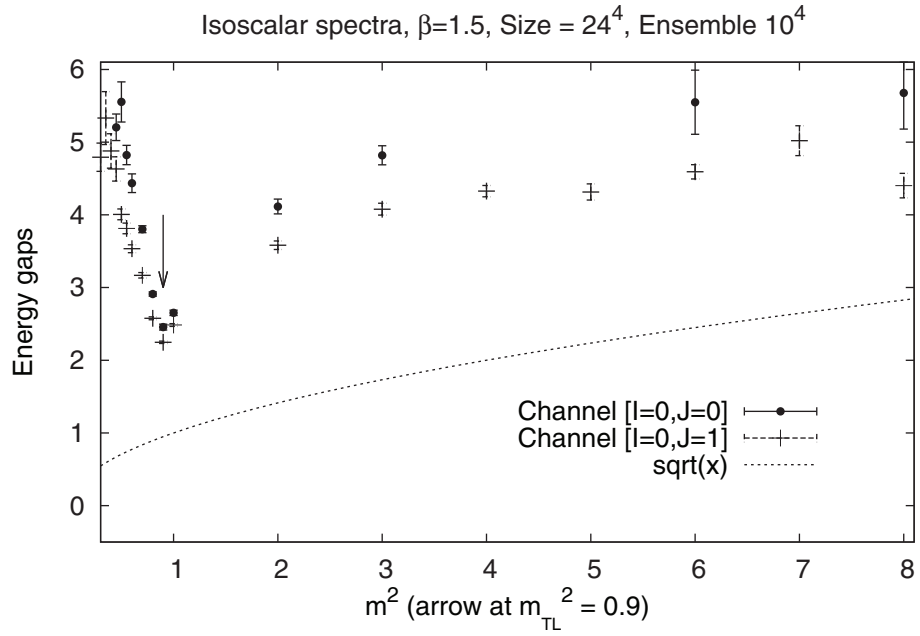

Fig. 5. – Mass spectrum in the isoscalar channels ($J = 0, 1$) for $\beta = 1.5$.

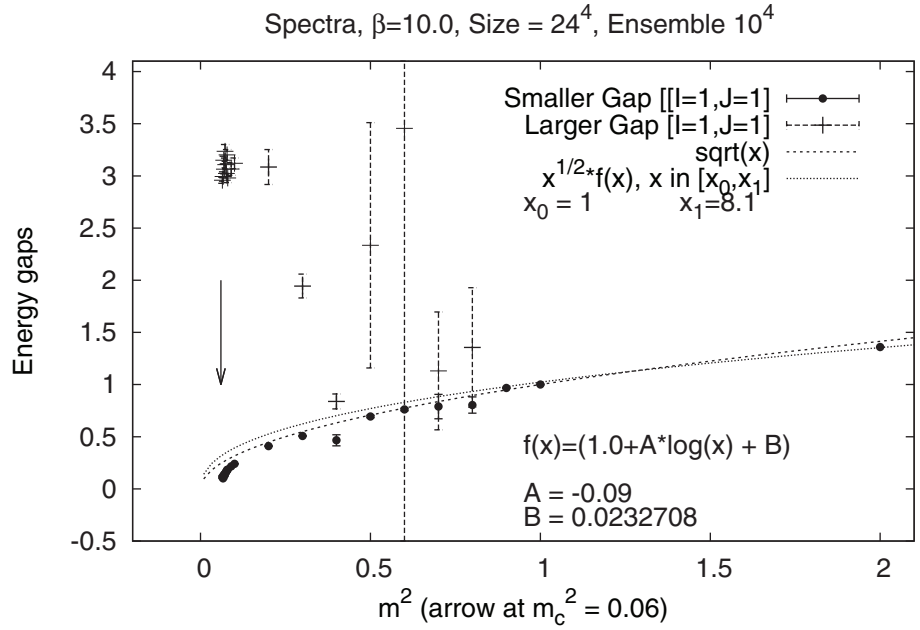

Fig. 6. – Mass spectrum in the isovector channel ($J = 1$) for $\beta = 10$.

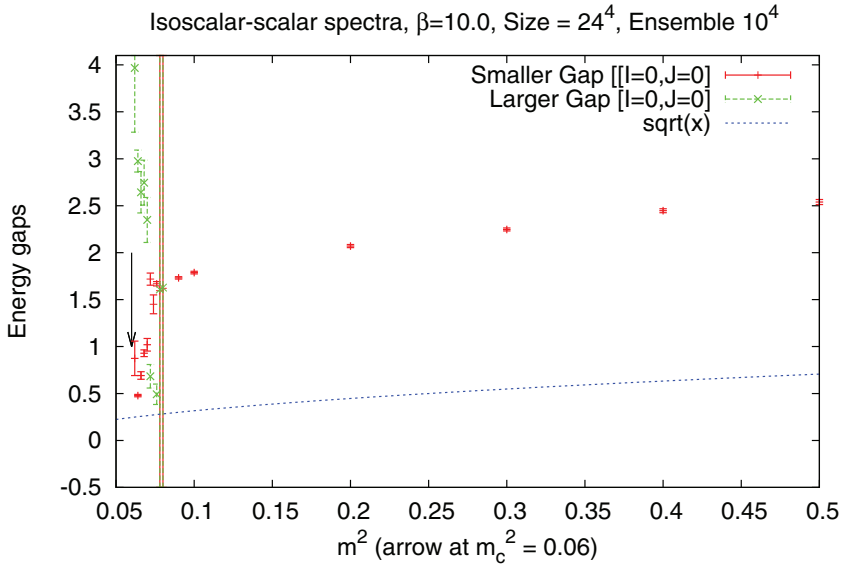

Fig. 7. – Mass spectrum in the isoscalar channel ($J = 0$) for $\beta = 10$.

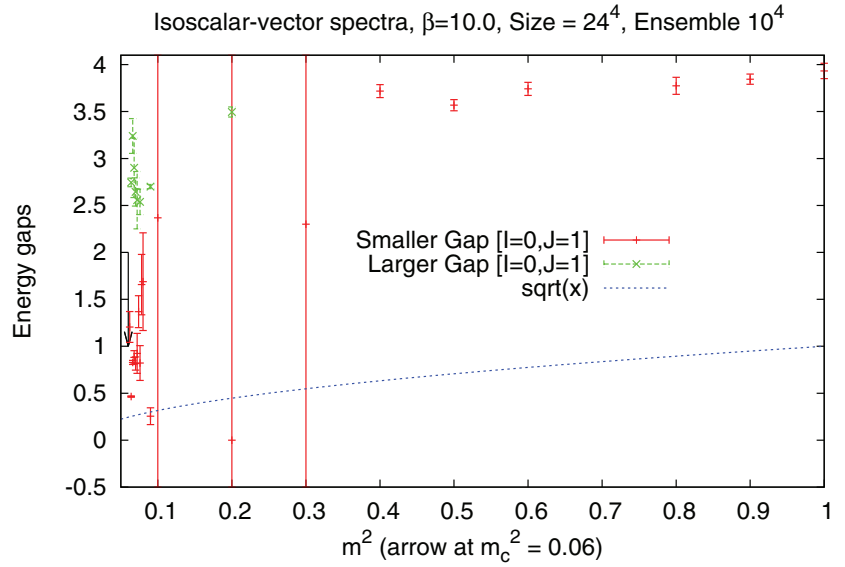

Fig. 8. – Mass spectrum in the isoscalar channel ($J = 1$) for $\beta = 10$.

REFERENCES

[1] Bettinelli D., Ferrari R. and Quadri A., *Phys. Rev. D*, **77** (2008) 045021.
[2] Bettinelli D., Ferrari R. and Quadri A., *Phys. Rev. D*, **77** (2008) 105012.
[3] Ferrari R., *JHEP*, **048** (2005) 0508.
[4] Ferrari R., *Acta Phys. Polon. B*, **43** (2012) 1965.
[5] Ferrari R., *Acta Phys. Polon. B*, **44** (2013) 1871.